Isospin-Forbidden Compound Nuclear Resonances in ^{25}Al and ^{29}P†*

B. TEITELMAN‡ AND G. M. TEMMER
Department of Physics, Rutgers–The State University, New Brunswick, New Jersey 08903

(Received 20 May 1968)

The analogs of the ground state and first excited state of ^{25}Na and ^{29}Al have been studied as compound resonances in ^{25}Al and ^{29}P, respectively, formed by scattering protons from ^{24}Mg and ^{28}Si targets. The accurate excitation energies obtained for these resonances, which are in excellent agreement with their locations available from delayed-proton, (p, t), and (p, γ) experiments, were used to predict the masses of ^{25}Si and ^{29}S from the isobaric-multiplet mass formula, and to calculate Coulomb-energy differences between the members of these isospin quartets. Total widths (<300 eV) and partial proton widths were extracted for the sharp isospin-forbidden $T=\frac{3}{2}$ resonances and compared with the widths of several new $T=\frac{1}{2}$ resonances in ^{25}Al and ^{29}P lying in the same region of excitation (7.5 to 10.0 MeV). Shifts are observed between the locations of corresponding analog states in the parent and $T_z=-\frac{1}{2}$ nuclei.

I. INTRODUCTION

In recent years much experimental, as well as theoretical, activity has been devoted to studying the properties of the analogs of the ground states and low-lying excited states of heavy nuclei with $T=T_z=\frac{1}{2}(N-Z)$ (the "parent" nuclei), observed as compound nuclear resonances in the nearest-neighboring member of the multiplet, namely, the nucleus with isospin projection $T_z'=T-1$. These analog resonances, with isospin $T_>=T$, lie at relatively high excitation energies in the heavy compound nuclei, amidst a sea of overlapping resonances with isospin $T_<=T-1$. When the level density of $T_<$ states is high enough, the $T_>$ analog resonances are found to stand out from a smoothly varying background in proton-scattering experiments, mainly because of their greater structural simplicity.

In the lighter nuclei this type of "conventional" analog-resonance experiment is not usually feasible, since it requires scattering from nuclei with $T=T_z=1$ or greater, and there are only a few of these which are stable. Moreover, in the light nuclei the proton-bombarding energies required are very low because of the energetic interplay of proton separation energy, symmetry energy, and Coulomb-displacement energy. We have, therefore, considered forming these resonances in the next-nearest neighbor, i.e. the member of the multiplet with isospin projection $T_z''=T-2$. In these cases the target nuclei are all stable, but the price to be paid is the violation of the isospin conservation law, since we scatter protons from targets with isospin $T-\frac{3}{2}$ so that the isospins of the channel and compound-nuclear wave functions differ by one or two units. In addition, in all the cases we have studied, all of the open exit channels also have isospin $T-1$ or $T-2$, so that *all* partial widths for the resonance involve violations of isospin conservation by one or two units (with the exception of the negligibly small γ-decay width); hence, the total width of the resonance will be exceedingly small. For example, for the $T=\frac{3}{2}$ resonances in ^{25}Al and ^{29}P ($T_z''=-\frac{1}{2}$) we scattered protons from the zero-isospin targets ^{24}Mg and ^{28}Si, respectively; the only open exit channels, besides elastic scattering, were inelastic scattering to the lower excited states of these targets, all of which had channel isospin $\frac{1}{2}$. To form the $T=2$ states in ^{12}C,[1] ^{16}O,[2] ^{20}Ne,[3] and ^{24}Mg[1] which originally aroused our interest in this type of experiment, we scattered protons from targets with isospin $\frac{1}{2}(T_z=\frac{1}{2})$—^{11}B, ^{15}N, ^{19}F, and ^{23}Na, respectively; the proton elastic and inelastic exit channels, as well as the neutron channels for ^{12}C and ^{16}O, have isospin 0 or 1, while the α-decay channels for these resonances have isospin 0, violating isospin conservation by two units. These early attempts were unsuccessful.

In undertaking a search for an isospin-forbidden resonance, we usually need to have some prior knowledge as to the location of the energy level. The $T=2$ states in $T_z=0$ nuclei were discovered as residual states in (p, t) and $(p, {}^3\mathrm{He})$ isospin-*allowed* two-nucleon pick-up reactions on $T=1$ targets.[2] The $T=\frac{3}{2}$ states in $T_z=-\frac{1}{2}$ nuclei which we studied were previously located by the isospin allowed $^{27}\mathrm{Al}(p, t)^{25}\mathrm{Al}$ and $^{31}\mathrm{P}(p, t)^{29}\mathrm{P}$ reactions,[4] as well as by detection of the "delayed" proton decays from these $T=\frac{3}{2}$ states following superallowed β^+ decay from ^{25}Si[5] and ^{29}S,[6] respectively, the $T_z=-\frac{3}{2}$ members of the quartets.

† Presented by B. Teitelman in partial fulfillment of the requirements for the Ph.D. degree at Rutgers University.

* Supported in part by the National Science Foundation.

‡ Present address: General Electric Company, Knolls Atomic Power Laboratory, Schenectady, N.Y. 12301.

[1] J. Cerny, Ann. Rev. Nucl. Sci. **18** (to be published).

[2] G. T. Garvey, J. Cerny, and R. Pehl, Phys. Rev. Letters **12**, 726 (1964); **13**, 548 (1964).

[3] C. A. Barnes (private communication to G. T. Garvey).

[4] J. C. Hardy and D. J. Skyrme, Bull. Am. Phys. Soc. **11**, 627 (1966); in *Isobaric Spin in Nuclear Physics*, edited by J. D. Fox and D. Robson (Academic Press Inc., New York, 1966), p. 701.

[5] R. McPherson and J. C. Hardy, Can. J. Phys. **43**, 1 (1965); J. C. Hardy and R. E. Bell, *ibid.* **43**, 1671 (1965); P. L. Reeder, A. M. Poskanzer, R. A. Esterlund, and R. McPherson, Phys. Rev. **147**, 781 (1966).

[6] J. C. Hardy and R. I. Verrall, Phys. Letters **13**, 148 (1964); T. H. Braid, A. M. Friedman, and R. W. Fink, Bull. Am. Phys. Soc. **10**, 120 (1965).

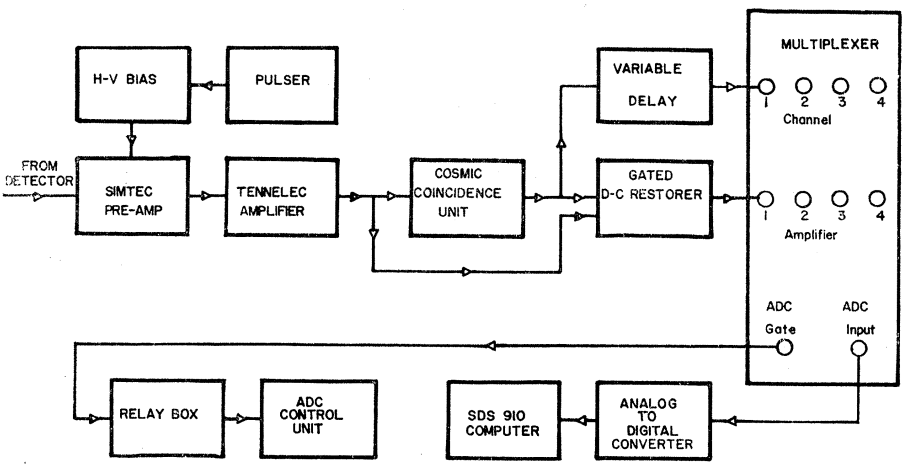

FIG. 1. Detection system electronics. Components without commercial manufacturer's label were designed and constructed at Rutgers or at Bell Telephone Laboratories, Murray Hill, N.J.

In this paper we shall present an analysis of cross-section measurements for proton elastic and inelastic scattering from ^{24}Mg and ^{28}Si to study the properties (especially the widths) of the analogs of the ground and first-excited states of ^{25}Na and ^{29}Al in ^{25}Al and ^{29}P, respectively. The appropriate region of excitation for the first $T=\frac{3}{2}$ states in ^{29}P had been covered by Brenner *et al.*,[7] but the 10-keV steps taken in the excitation curve were too coarse to observe the narrow $T=\frac{3}{2}$ resonance. These data terminated at a proton energy of 7.00 MeV, below the region of the *second* $T=\frac{3}{2}$ state in ^{29}P; we therefore extended the excitation curve up to 7.43 MeV, discovering several new, isospin-allowed $T=\frac{1}{2}$ resonances in the process. The published elastic proton-scattering cross sections on ^{24}Mg [8] ended at 4.0 MeV, so that we had to cover a 600-keV region of excitation (in 5-keV steps) in the neighborhood of the $T=\frac{3}{2}$ resonances at about 5.9 MeV, again uncovering several new $T=\frac{1}{2}$ resonances.

We wish to take note here of other workers in the field who have made recent contributions to the study of isospin-forbidden, compound-nuclear resonances. Resonant proton-capture experiments on ^{24}Mg and ^{28}Si by Youngblood *et al.*[9] have yielded radiative widths for the $T=\frac{3}{2}$ resonances in ^{25}Al and ^{29}P, whose locations are found to be in excellent agreement with our values for the excitation energies. Furthermore, $T=\frac{3}{2}$ resonances in the $T_z=-\frac{1}{2}$ nuclei ^{13}N,[10] ^{17}F,[11] ^{21}Na,[12] ^{37}K,[13] and ^{41}Sc [14] have now been observed by proton scattering from ^{12}C, ^{16}O, ^{20}Ne, ^{36}Ar, and ^{40}Ca, respectively.

Note added in manuscript: Very recently, the $T=\frac{3}{2}$ resonance in ^{33}Cl by proton scattering from ^{32}S was also found [G. Poiani, R. A. Ricci, *et al.*, and R. Van Bree, (private communications)].

Detailed reports on the former two nuclei are in preparation at Rutgers.[15] Thus a large body of information on isospin-forbidden $T=\frac{3}{2}$ resonances in the light nuclei is accumulating from which systematic conclusions as to isospin impurities introduced by the Coulomb interaction between protons are becoming possible. It has not been necessary so far to discard the concept of charge independence for the specifically nuclear interactions.

II. EXPERIMENTAL DETAILS

The important requirements for the success of these experiments were determined by the extremely narrow total widths of these resonances (of the order of 90–210 eV). This restricted the tolerable spread in beam energy and target thickness to no more than a few keV, and also demanded that the beam energy be changed in small steps, typically 1 keV. The required proton beam was provided by the Rutgers tandem Van de Graaff accelerator,[16] capable of producing variable-energy proton beams from 2 to 17 MeV, with beam spreads held to within ± 1.5 keV.[17] The targets were thin films of Mg and Si, evaporated by ohmic heating onto thin carbon backings[18] (see Appendix A).

A collimated proton beam was focused onto the target in the center of a 43-cm-diam ORTEC[19] scattering

[7] M. W. Brenner, A. M. Hoogenboom, and E. Kashy, Phys. Rev. **127**, 947 (1962).
[8] F. P. Mooring, L. J. Koester, E. Goldberg, D. Saxon, and S. G. Kaufmann, Phys. Rev. **84**, 703 (1951).
[9] D. H. Youngblood, G. C. Morrison, and R. E. Segel, Phys. Letters **22**, 625, (1966); G. C. Morrison, D. Youngblood, R. C. Bearse, and R. E. Segel, J. Phys. Soc. Japan Suppl. **24**, 653 (1968).
[10] D. J. Bredin, O. Hansen, G. M. Temmer, and R. Van Bree, in *Isobaric Spin in Nuclear Physics*, edited by J. D. Fox and D. Robson (Academic Press Inc., New York, 1966), p. 472.
[11] R. Van Bree and G. M. Temmer, Bull. Am. Phys. Soc. **12**, 518 (1967); J. R. Patterson, H. Winkler and C. S. Zaidins, Phys. Rev. **163**, 1051 (1967).
[12] A. B. McDonald, J. R. Patterson, and H. Winkler, Bull. Am. Phys. Soc. **13**, 625 (1968).
[13] D. R. Goosman and R. W. Kavanagh, Phys. Rev. **161**, 1156 (1967); D. R. Goosman, *ibid.* **163**, 1219 (1967).
[14] D. H. Youngblood, B. H. Wildenthal, and C. M. Class, Phys. Rev. (to be published); see also, Ref. 22.
[15] R. Van Bree and G. M. Temmer (unpublished).
[16] Purchased from High Voltage Engineering Corp., Burlington, Mass.
[17] E. A. Gere, H. P. Lie, and G. L. Miller, Bull. Am. Phys. Soc. **12**, 943 (1967).
[18] Purchased from Yissum Research Development Co., Jerusalem, Israel.
[19] Purchased from Oak Ridge Technical Enterprises Corp., Oak Ridge, Tenn.

TABLE I. Excitation energies (MeV) of $T=\frac{3}{2}$ states.

State	Present work	Delayed-proton emitters	(p,t)	(p,γ)
^{25}Al, 1st	7.916±0.006[a]	7.93±0.02[b]	7.914±0.025[c]	7.914±0.010[d]
^{25}Al, 2nd	7.987±0.006[a]			7.983±0.010[d]
^{29}P, 1st	8.376±0.006[a]	8.36±0.03[e]	8.361±0.035[c]	8.374±0.010[d]

[a] Reference 25.
[b] Reference 5.
[c] Reference 4.
[d] Reference 9.
[e] Reference 6

chamber. A Faraday cup placed about 1 m behind the chamber was used to collect the incident charge, which was measured using a sensitive feed-back current integrator.[20] Scattered protons were detected with solid-state detectors[21] with 2-mm depletion depth. Typical detector resolutions were about 50 keV for 6-MeV protons, which was sufficient to resolve the elastic peaks from impurity peaks, and to resolve the inelastic peaks from each other.

A schematic diagram of the detection system electronics is shown in Fig. 1. Pulses from the detector were digitized, after amplification and pulse shaping, in an analog-to-digital converter for storage in the memory of our on-line SDS 910 computer. This computer, as well as an off-line SDS 925 computer, provided considerable flexibility in processing the raw pulse-height data to provide differential cross sections in the center-of-mass system.

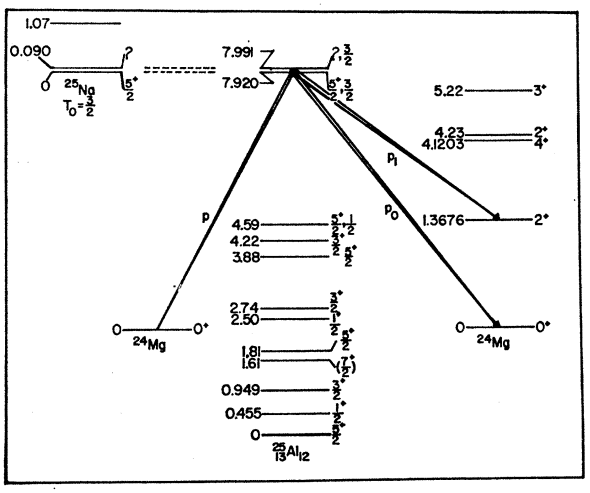

FIG. 2. Level diagram for ^{25}Al showing five bound states and some of the unbound $T=\frac{1}{2}$ levels. Levels in the parent nucleus ^{25}Na, corresponding to the $T=\frac{3}{2}$ resonances, are indicated, as well as the proton-decay channels observed for the resonances.

[20] Purchased from E. J. Rogers, Co., Brookhaven, N.Y.
[21] Purchased from Technical Measurements Corp., San Mateo, Calif.

III. $T=\frac{3}{2}$ RESONANCES IN ^{25}Al

The level diagram for ^{25}Al, as shown in Fig. 2, consists of five bound levels, followed by many unbound $T=\frac{1}{2}$ states[22] (not all of which are shown in the diagram); not until we reach an excitation energy of 7.920 MeV do we find the first level with $T=\frac{3}{2}$, which is the analog of the ground state of ^{25}Na—the parent of the mass-25 quartet. We attempted to observe this first $T=\frac{3}{2}$ state as a resonance in the compound nucleus formed by bombarding ^{24}Mg with protons, and detecting both the elastically and inelastically scattered protons, as shown in a typical pulse-height spectrum for a Mg target (Fig. 3). Excitation curves in 1-keV steps over the appropriate incident proton energies for the ^{25}Na ground-state-analog resonance are shown in Figs. 4–8, at laboratory angles of 88.0°, 123.3°, 148.1°, and 165.0°, respectively. Because of the extremely narrow width of this resonance (~90 eV), the resonant excursion was always observed to be <15% of $d\sigma/d\Omega$ (average) and was stronger in the first inelastic channel than in elastic scattering.[6] As we continued these excitation

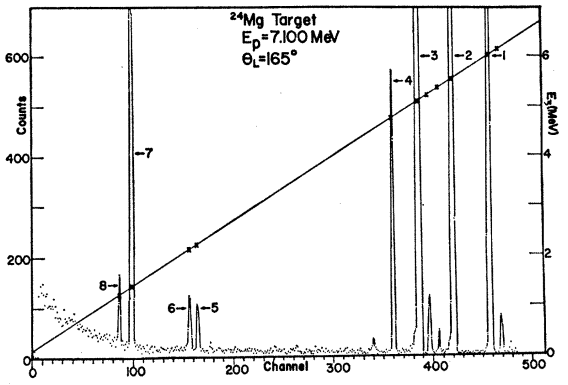

FIG. 3. Proton pulse-height spectrum for a Mg target. Peak identification: (1) ^{24}Mg elastic; (2) ^{16}O elastic; (3) ^{12}C elastic; (4) ^{24}Mg (1.3676 MeV, 2^+); (5) ^{24}Mg (4.1203 MeV, 4^+); (6) ^{24}Mg (4.23 MeV, 2^+); (7) ^{12}C (4.433 MeV, 2^+); (8) ^{24}Mg (5.22 MeV, 3^+). Unlabeled peaks are impurities; left-hand ordinate-counts; right-hand ordinate-scattered-proton energy.

[22] P. M. Endt and C. Van der Leun, Nucl. Phys. A105, 1 (1967).

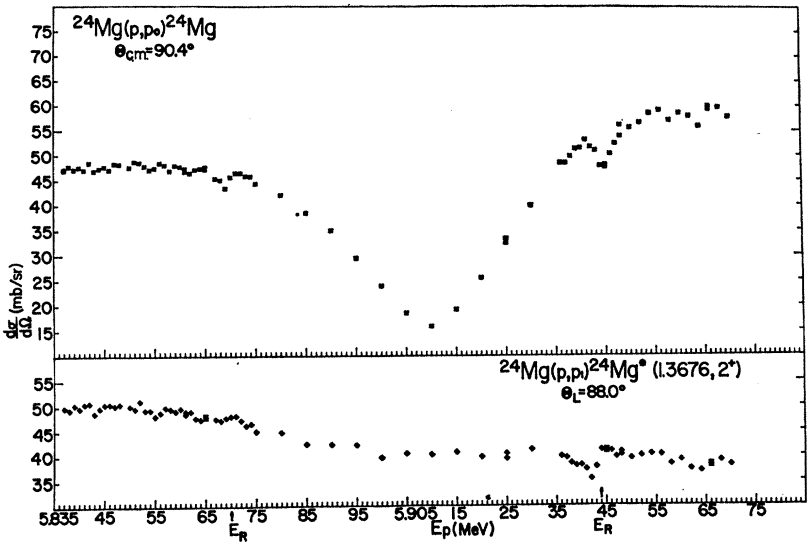

FIG. 4. Excitation curves at 88° for elastic and inelastic proton scattering to the 1.37 MeV, 2^+ state in ^{24}Mg. Sharp $T=\frac{3}{2}$ resonances at 5.870 and 5.944 MeV (indicated by arrows) are separated by a $T=\frac{1}{2}$ resonance which does not resonate in the inelastic channel. Dips in the elastic excitation curve at 90° (c.m.) indicate $l_p \neq 1$. 1-keV steps near analog resonances, 5-keV steps elsewhere. Cross sections in c.m. system; E_p in lab system.

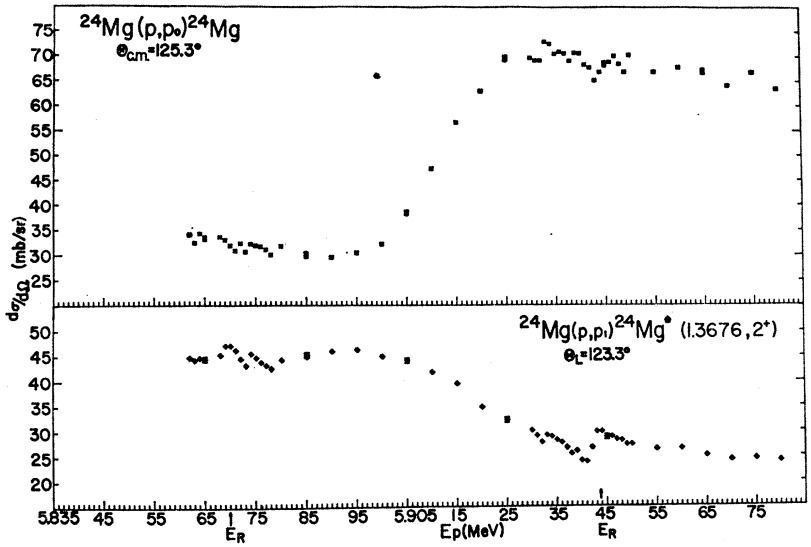

FIG. 5. Excitation curves at 123.3° (lab) for elastic and inelastic proton scattering from ^{24}Mg. Note appearance of $T=\frac{1}{2}$ resonance (at ~5.91 MeV) in the inelastic channel and suppressed zeros for the cross section (c.m.) scale. Arrows indicate $T=\frac{3}{2}$ resonances. Proton energies in the lab system.

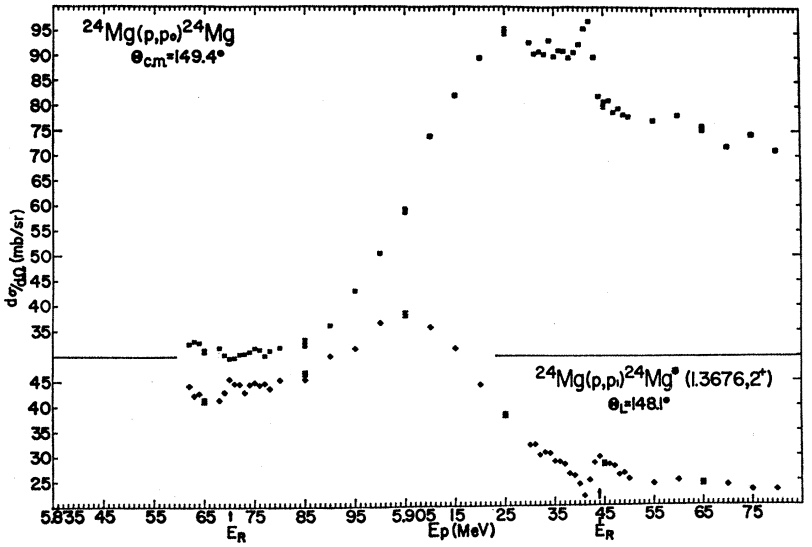

FIG. 6. Excitation curves at 148.1° (lab) for elastic and inelastic proton scattering from ^{24}Mg. Resonance excursions are largest at this angle. Arrows indicate $T=\frac{3}{2}$ resonances. Cross sections in c.m. system; E_p in lab system.

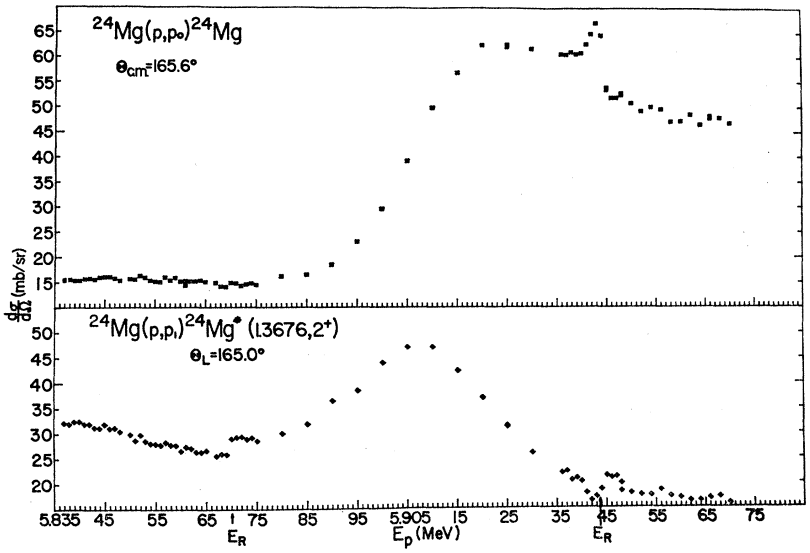

FIG. 7. Excitation curves at 165.0° (lab) for elastic and inelastic proton scattering from ^{24}Mg. Note absence of ^{25}Na ground-state analog resonance in the elastic channel. Branching ratio consistent with that obtained from delayed-proton emitter ^{25}Si (Ref. 5). Arrows indicate $T=\frac{3}{2}$ resonances. Cross sections in c.m. system, E_p in lab system.

curves, we passed over a typical $T=\frac{1}{2}$ resonance with total width of 35±10 keV, until we reached the region of excitation corresponding to the analog of the first-excited state of ^{25}Na in ^{25}Al. Notice that although the first-excited state lies at an excitation energy of 90 keV (in the parent), the separation between the analog resonances is only 71 keV. The explanation of this discrepancy may be found in the Coulomb perturbation of the energy levels, which is also responsible for the isospin mixing process and will be discussed later. Our results for the excitation energies of these $T=\frac{3}{2}$ levels are in excellent agreement with other determinations, as listed in Table I. Preliminary results for these $T=\frac{3}{2}$ resonances in ^{25}Al have been reported.[23–25] The second $T=\frac{3}{2}$ resonance in ^{25}Al is presumed to have spin $\frac{3}{2}^+$, since its γ-decay branching is 82% to the $\frac{5}{2}^+$ ground state, and 18% to the $\frac{1}{2}^+$ first-excited state of ^{25}Al, indicating a $\frac{3}{2}^+$ assignment for an $M1$-type transition.[9]

IV. $T=\frac{3}{2}$ RESONANCES IN ^{29}P

A level diagram for ^{29}P, as shown in Fig. 9, reveals four bound states, followed by many unbound $T=\frac{1}{2}$ levels, many of which have been observed as resonances[7,26]; at an excitation energy of 8.380 MeV we find the analog of the $\frac{5}{2}^+$ ground state of ^{29}Al in ^{29}P. At the appropriate proton energy to excite this first $T=\frac{3}{2}$

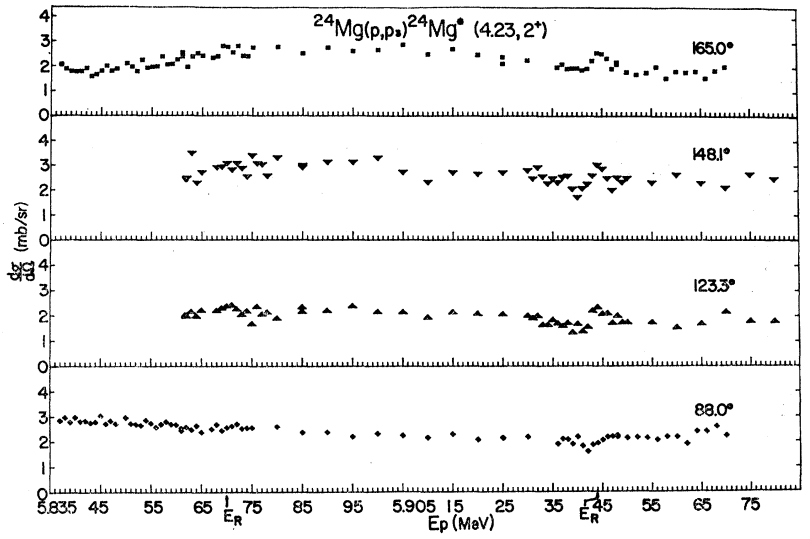

FIG. 8. Excitation curves for inelastic proton scattering to ^{24}Mg (4.23 MeV, 2$^+$) state. Note absence of $T=\frac{1}{2}$ resonance in this channel. Second $T=\frac{3}{2}$ state shows definite resonance effect. Arrows indicate $T=\frac{3}{2}$ resonances. Cross sections in c.m. system, E_p in lab system.

[23] G. M. Temmer and B. Teitelman, Bull. Am. Phys. Soc. **12**, 554 (1967).
[24] G. M. Temmer, B. Teitelman, R. Van Bree, and H. Ogata, J. Phys. Soc. Japan Suppl. **24**, 299 (1968).
[25] B. Teitelman and G. M. Temmer, Phys. Letters **26B**, 371 (1968); **27B**, 18 (1968).
[26] T. A. Belote, E. Kashy, and J. R. Risser, Phys. Rev. **122**, 920 (1961).

TABLE II. Widths for the $T=\frac{3}{2}$ resonances in ^{25}Al and ^{29}P.

Parent state	$\theta_{C.M.}$ (deg)	δ [a] (keV)	τ [b] (keV)	A mb/sr	B mb/sr	γ (deg)	Γ_p/Γ	Γ (eV)
^{25}Na (g.s.)	...	1.0	0.8	...	...	...	0.17[c]	90±80[d]
^{25}Na (0.090)	165.6	1.0	0.8	30.0	93.52	32.5	0.50[e]	182
	149.4	1.0	0.8	61.5	74.47	35.0	0.50	258
	90.4	1.0	0.8	18.0	36.3	94.2	0.50	192
							Average	211±50
^{29}Al (g.s.)	165.5	1.5	2.0	30.0	330.0	27.0	0.80[f]	143
	90.0	1.5	2.0	5.7	90.67	125.0	0.80	192
							Average:	168±50

[a] Beam spread.
[b] Target thickness.
[c] Based on Ref. 5.
[d] Estimated value.
[e] Estimated from comparisons of elastic and inelastic yields.
[f] Based on Ref. 6.

resonance, only elastically scattered and inelastically scattered protons to the 2^+ first excited state of ^{28}Si are seen above the background, as shown in Fig. 10. Excitation curves for these two channels over the ^{29}Al ground-state analog resonance are shown in Figs. 11 and 12. A discussion of the analog of the first-excited 1.406-MeV state of ^{29}Al in ^{29}P will be given later. Preliminary results for these $T=\frac{3}{2}$ resonances in ^{29}P have been reported.[24,25,27]

V. TOTAL AND PARTIAL PROTON WIDTHS OF $T=\frac{3}{2}$ RESONANCES

The sharpness of the isospin-forbidden resonances under study provided some complications, but also simplifications, in the extraction of the total and partial proton widths from the cross-section measurements. Making the assumption that the nonresonant portions of the elastic-scattering amplitudes are energy-independent as we pass through a narrow resonance allowed us to simplify the theoretical expression for the cross section to the form[28]

$$d\sigma/d\Omega = A + B\sin^2(\beta+\gamma),$$

where the resonant phase $\beta = \tan^{-1}\Gamma/2/(E_R-E)$; A, B, and γ are constants, and E_R and Γ are the resonant energy and total width, respectively. Furthermore, the ratio Γ_p/Γ may be expressed in terms of these constants; *a priori* knowledge of this ratio in the case of ground-state analog resonances from delayed-proton branching ratio measurements,[5,6] or estimates from the inelastic-scattering data for the first excited state analog resonances, along with knowledge of the off-resonant cross sections, allowed us to uniquely determine A, B, and γ. However, before we could compare the theoretical and experimental cross sections in order to extract Γ, we had to average the theoretical expression to take into account the effects of imperfect beam-energy resolution. We assumed an energy-distribution function of triangular shape for the beam-energy spread appropriate for a magnetically analyzed beam passing through narrow image slits, and of square shape for energy losses in the target. Since formulas for the combined effects of these spreading mechanisms were not explicitly available in the literature for the general case, they are derived in Appendix B. Our procedure was to find the value of Γ which minimized

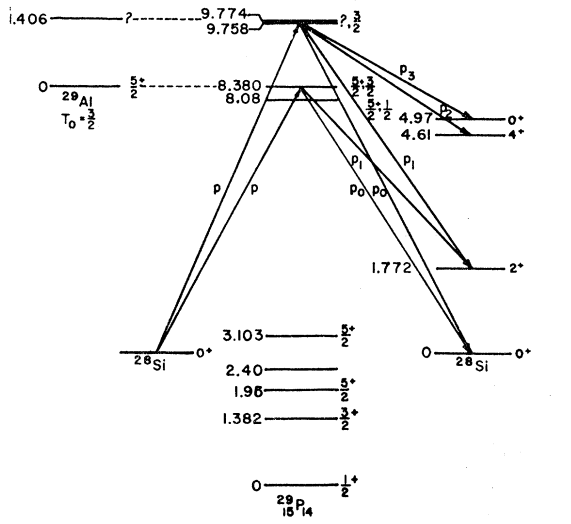

FIG. 9. Level diagram for ^{29}P showing four bound states and two unbound $T=\frac{1}{2}$ levels. The first excited, 1.406-MeV state of ^{29}Al probably has a spin $\frac{1}{2}^+$; this eliminates either of the states at 9.758 or 9.774 MeV in ^{29}P as analog state candidates since both have $l_p=2$. Exit channels are also indicated.

[27] B. Teitelman, J. P. F. Sellschop, G. M. Temmer, and G. T. Garvey, Bull. Am. Phys. Soc. **12**, 570 (1967).
[28] E.g., H. T. Richards, in *Nuclear Spectroscopy* edited by F. Ajzenberg-Selove (Academic Press Inc., New York, 1960), Part A, p. 99.

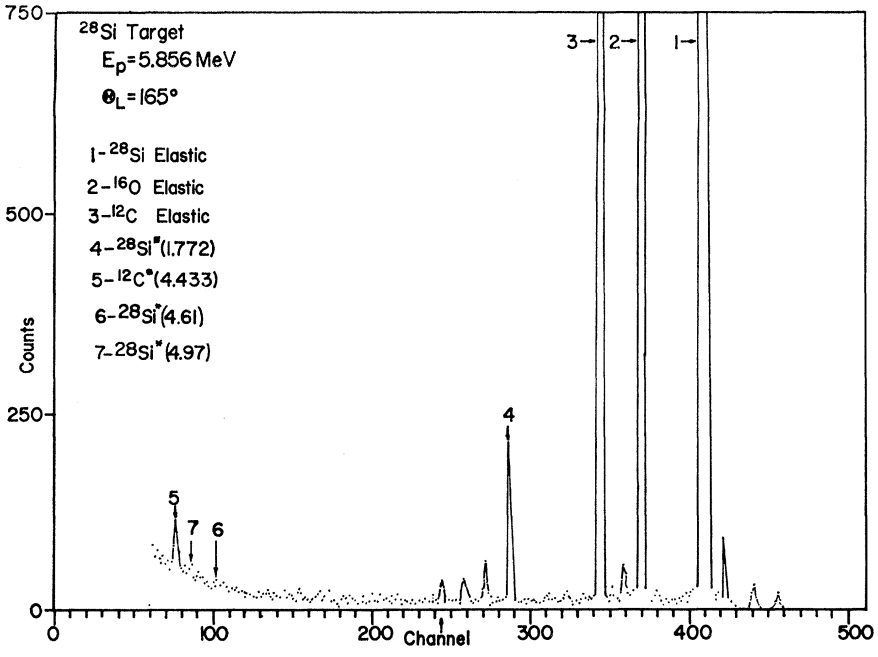

FIG. 10. Pulse-height spectrum for a Si target. Although above threshold for excitation of the ^{28}Si* (4.61) and ^{28}Si* (4.97) states, they are not seen above background at this proton energy. Small peaks in this spectrum are from ^{29}Si, ^{30}Si, and other impurities.

TABLE III. $T=\frac{1}{2}$ resonances in ^{25}Al.

E_p [a] (MeV)	E_x (MeV)	Γ (keV)	Observed in inelastic scattering: (1.3676, 2^+)	(4.1203, 4^+)	(4.23, 2^+)	Probable l_p
5.601	7.662	50±15	x		x	3
5.811	7.863	20±8	x	x		1
5.903	7.951	35±10	x	x		2
5.996	8.041	20±10			x	2
6.056	8.098	15±7	x	x	x	2
6.171	8.209	40±10	x		x	0

[a] Resonant energies based on corrected calibration which unfortunately differs from the energy scale of some of the graphs.

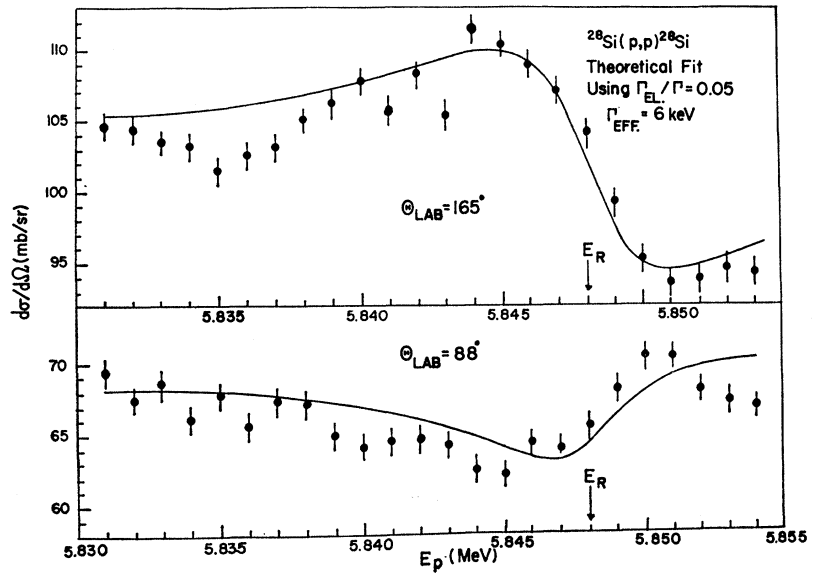

FIG. 11. Ground-state analog of ^{29}Al in ^{29}P, elastic channel. Theoretical fit uses unaveraged expression for cross section. Γ_{eff} consists almost entirely of beam spread and target thickness. True width is about 170 eV. When repeated with thinner targets, resonance excursion increases while Γ_{eff} decreases.

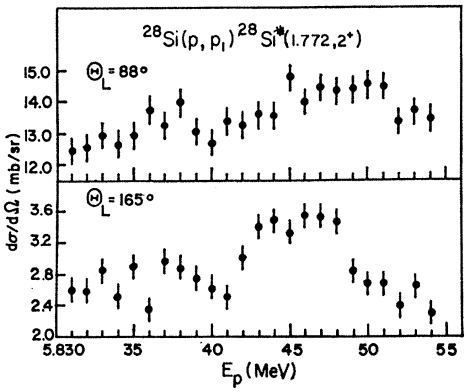

FIG. 12. Ground-state analog of ^{29}Al in ^{29}P, first inelastic channel. Note absence of resonance at 88°, and suppressed zeros. $\Gamma_{p'}/\Gamma \cong 0.2$. Cross section in c.m. system, E_p in lab system.

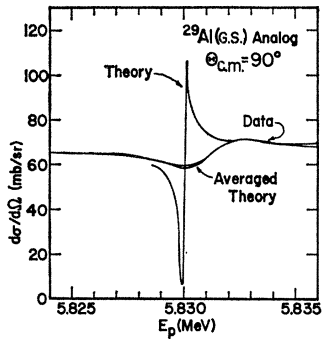

FIG. 14. Fit to the ^{29}Al (g.s.) analog resonance at 90° (c.m.). Curve labeled "Theory" is plot of function

$$d\sigma/d\Omega = 5.7 + 90.67 \sin^2(\beta + 125°),$$

where $\beta = \tan^{-1}[\frac{1}{2}0.000192/(5.830 - E)]$.

the χ^2 function between the experimental and averaged theoretical cross sections. Examples of typical fits obtained by this procedure are shown in Figs. 13 and 14 for the ground-state analog of ^{29}Al in ^{29}P. A summary of the total and partial widths we have extracted for these sharp resonances is provided in Table II. The quoted experimental errors arise mainly from uncertainties in our knowledge of the beam spread (δ) and target thickness (τ), and were assigned by repeating our computer search for the width Γ using different input values for δ and τ. The beam spread was estimated from the known accelerator terminal ripple (± 1 kV) and by observing the spreading effects on several known narrow ^{28}Si+p resonances[26] at lower incident proton energies; the target thickness was calculated by measuring the number of scattered protons corresponding to a known differential cross section and measuring the incident beam current and detector solid angle. It should be borne in mind, however, that the best previous width determinations were *upper limits* placed by detector resolution—usually no less than 80 keV.

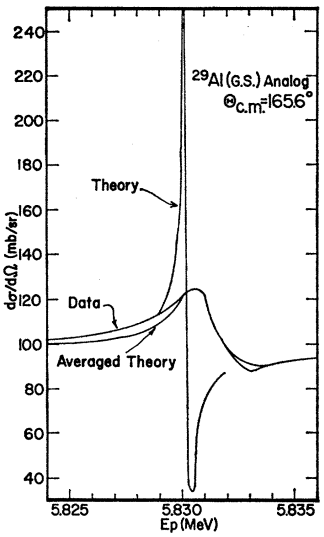

FIG. 13. Fit to the ^{29}Al (g.s.) analog resonance at 165.6° (c.m.) illustrating the effects of averaging over the beam energy distribution. Curve labeled "Theory" is plot of function $d\sigma/d\Omega = 30 + 330 \sin^2(\beta + 27°)$, where $\beta = \tan^{-1}[\frac{1}{2}0.000143/(5.830 - E)]$.

VI. NEW $T = \frac{1}{2}$ RESONANCES IN ^{25}Al AND ^{29}P

In the course of these investigations of sharp states we have covered some previously unexplored regions of the proton elastic and inelastic scattering excitation curves on ^{24}Mg and ^{28}Si. These are shown at two angles for a ^{24}Mg target in Figs. 15–17, and at three angles for a ^{28}Si target in Figs. 18–22. The correlated peaks observed in the excitation curves at different angles and for different channels represent, we believe, individual compound-nucleus resonances superimposed, perhaps, on a direct reaction background.[29] We have extracted incident proton and excitation energies, and total widths for these resonances as listed in Tables III

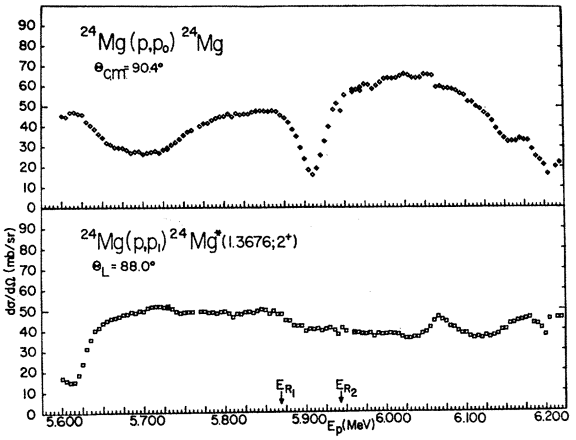

FIG. 15. 5-keV step excitation curves at 88° (lab) for proton elastic and inelastic (2^+) scattering from ^{24}Mg. Arrows along abscissa indicate positions of sharp $T = \frac{3}{2}$ resonances. Note large direct-reaction contribution to the inelastic cross sections.

[29] F. D. Seward, Phys. Rev. **114**, 514 (1959).

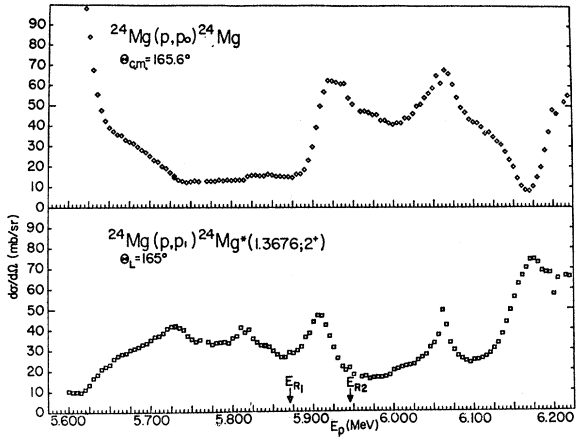

FIG. 16. 5-keV step excitation curves at 165° (lab) for ^{24}Mg(p, p_0) and ^{24}Mg(p, p_1). Several distinct, but overlapping, $T=\frac{1}{2}$ resonances are discernible in the inelastic excitation curve. Individual resonances are more difficult to distinguish in the elastic excitation curve.

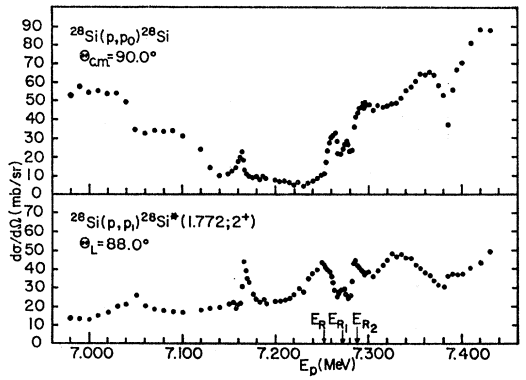

FIG. 18. Excitation curves at 88° (lab) in the vicinity of the second $T=\frac{3}{2}$ state in ^{29}P (predicted to lie at 7.298 MeV). Arrows labeled E_{R_1} and E_{R_2} indicate positions of two sharp resonances once thought to be candidates for the analog state (later analysis showed both of them to have the wrong l_p; see text). Arrow labeled E_R indicates surviving $T=\frac{3}{2}$ candidate.

and IV. Probable l values have been assigned to these resonances by consideration of the penetrabilities involved for decay to the excited 0^+, 2^+, and 4^+ states of the target nuclei. (For example, a strong yield to a 4^+ state indicates high compound-nucleus angular momentum J, whereas a strong yield to an excited 0^+ state indicates low J.) In elastic scattering at 90° (c.m.) a rise indicates odd l, whereas a dip indicates even l. The shapes at other angles for elastic scattering helped to remove any remaining ambiguities. The $T=\frac{1}{2}$ level in ^{25}Al at an excitation energy of 8.20 MeV seen by proton emission following allowed β^+ decay from ^{25}Si [5] seems to correspond in its decay properties to our level at 8.098 MeV, but with an energy discrepancy of 100 keV.

Several states in the corresponding excitation region of the mirror nucleus ^{29}Si of ^{29}P have been observed by

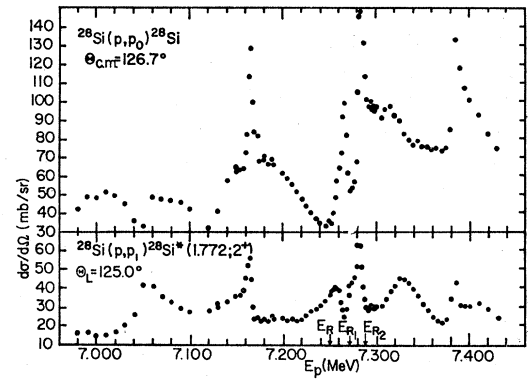

FIG. 19. Excitation curves at 125° (lab) in the vicinity of the second $T=\frac{3}{2}$ state in ^{29}P. Note several distinct $T=\frac{1}{2}$ resonances in the elastic and inelastic channels. Arrows labeled E_{R_1} and E_{R_2} indicate unsuccessful candidates for the analog state; E_R indicates the remaining candidate.

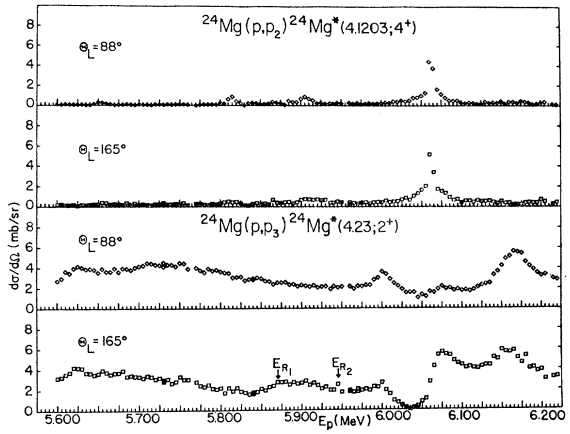

FIG. 17. 5-keV step excitation curves for the ^{24}Mg(4.1203,4$^+$) and ^{24}Mg(4.23,2$^+$) states. Note that cross sections to the 4^+ state are appreciable only on resonance, and that resonances appearing in the 2^+ excitation curve are absent in the 4^+ curve and vice versa, because of differences in the penetrabilities for decay to these states.

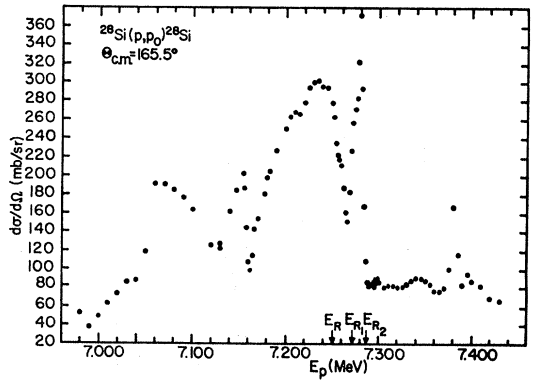

FIG. 20. Excitation curves at 165° (lab) in the vicinity of the second $T=\frac{3}{2}$ state in ^{29}P for the elastic channel. Note large excursion of several of the $T=\frac{1}{2}$ resonances Arrows labeled E_{R_1} and E_{R_2} indicate unsuccessful candidates for the analog state; E_R indicates remaining candidate.

TABLE IV. $T=\frac{1}{2}$ resonances in ^{29}P.

E_p [a] (MeV)	E_x (MeV)	Γ_{obs} (keV)	Observed in inelastic scattering: (1.772, 2^+)	(4.61, 4^+)	(4.97, 0^+)	Probable l_p
7.046	9.540	50±10	x		x	0
7.126	9.617	40±10	x		x	0
7.162	9.652	9±3	x	x		3
7.248[b]	9.735	7±3	x		x	0
7.266	9.753	8±3	x	x	x	2
7.279	9.765	8±3	x	x	x	2
7.322	9.807	20±10	x	x	x	2
7.381	9.864	12±5	x	x		2

[a] Resonant energies based on corrected calibration.
[b] Candidate for second $T=\frac{3}{2}$ state.

Hansen[30] in the ^{27}Al(^{3}He, p)^{29}Si reaction; by adjusting the energy scales so that the first $T=\frac{3}{2}$ states in these mirror nuclei lie at the same excitation energy (involving a shift of 82 keV upwards in the ^{29}Si scale) we find that most of the levels seen in ^{29}Si correspond to levels in ^{29}P; this is illustrated in Table V.

VII. PROBLEM OF THE ANALOG OF THE 1.406-MeV FIRST EXCITED STATE OF ^{29}Al

An example of the difficulties and pitfalls involved in determining the isospin of a compound nuclear resonance is provided by the second $T=\frac{3}{2}$ state in ^{29}P. At the start of our investigation the only information available on the levels of ^{29}Al was from the ^{27}Al(t, p)^{29}Al reaction of Jaffe *et al.*[31] No spin assignments had been made to any of the excited states of ^{29}Al. Our first search for the analog of the first excited state of ^{29}Al in ^{29}P was in the immediate region of 1.406 MeV above the excitation energy of the ground-state analog resonance; upon finding two narrow resonances at proton energies of 7.266 and 7.279 MeV, one 28 keV and the other 15 keV below the predicted location, we felt that either or both of these resonances could have isospin $\frac{3}{2}$. Hansen,[30] at our behest, performed a high resolution ^{26}Mg(α, p)^{29}Al experiment which showed conclusively that the parent state was *not* a doublet; thus either one, or neither, but not *both*, of these sharp resonances could be the analog of the ^{29}Al (1.406-MeV) state. In order to determine the spin of this level, Bearse *et al.*[32] analyzed angular distributions from the ^{30}Si(d, ^{3}He)^{29}Al reaction, using the DWBA code JULIE; they confirmed the $\frac{5}{2}^+$ assignment to the ground state of ^{29}Al, but concluded that the first-excited state had $l_p=0$ and hence spin $\frac{1}{2}^+$. Furthermore, Dehnhard *et al.*[33] performed the isospin-allowed neutron-pickup reaction ^{30}Si(^{3}He, α)^{29}Si and tentatively located the second $T=\frac{3}{2}$ state in ^{29}Si at an excitation of 1.34±0.01 MeV above the first $T=\frac{3}{2}$ state, with a $\frac{1}{2}^+$ assignment to this mirror level of the second $T=\frac{3}{2}$

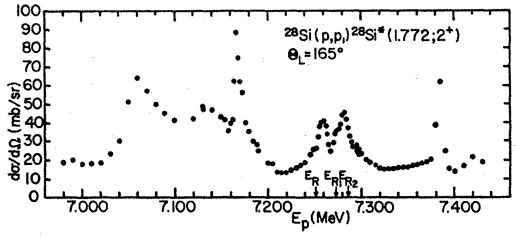

FIG. 21. First inelastic excitation curve at 165° (lab) in the vicinity of the second $T=\frac{3}{2}$ state in ^{29}P. Arrows labeled E_{R_1} and E_{R_2} indicate unsuccessful candidates for the analog state; E_R indicates remaining candidate.

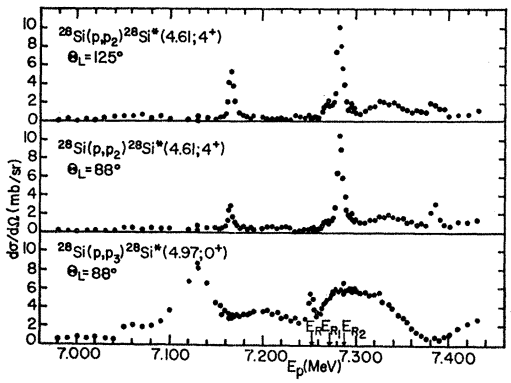

FIG. 22. States of ^{29}P decaying to the ^{28}Si(4.61,4^+) and ^{28}Si(4.97,0^+) channels. Resonance at $E_p=7.252$ MeV (arrow labeled E_R) decays strongly in the 0^+ channel, but is absent in the 4^+ channel indicative of a $\frac{1}{2}^+$ compound resonance. It therefore is the only candidate in this energy range to be the analog of the first excited, 1.406-MeV state of ^{29}Al. Unsuccessful candidates are indicated by arrows labeled E_{R_1} and E_{R_2}.

[30] O. Hansen (private communication)
[31] A. A. Jaffe, F. De S. Barros, P. D. Forsyth, J. Muto, I. J. Taylor, and S. Ramavataram, Proc. Phys. Soc. (London) **76**, 914 (1960).
[32] R. E. Bearse, D. H. Youngblood, and J. L. Yntema, Phys. Rev. **167**, 1043 (1968).
[33] D. Dehnhard and J. L. Yntema (private communication); and Phys. Rev. **163**, 1198 (1967).

TABLE V. Corresponding levels in ^{29}Si and ^{29}P.

E_x in ^{29}Si [a] keV	"E_x" in ^{29}Si [b] keV	E_x in ^{29}P [c] keV	Resonance in ^{29}P (MeV)	Reference	Comments
8 294	0	8 376	8.376	d	^{29}Al(gs) analog; $l_p=2$
8 555	261	8 637	8.62	e	$\Gamma\sim10$ keV
8 846	552	8 928	8.96	e	$\Gamma\sim50$ keV
9 046	752	9 128			
9 207	913	9 289	9.28	e	$\Gamma=7\pm3$ keV
9 291	997	9 373	9.37	e	$\Gamma=13\pm5$ keV
9 634	1340[f]	9 716	9.735	g	Surviving candidate for ^{29}Al (1.406 MeV) analog
9 685	1391	9 767	9.765	g	Second member of "doublet"; $l_p=2$
10 057	1763	10 139			Possibly ^{29}Al (1.76 MeV) analog

[a] Approximate excitation energies from ^{27}Al(^{3}He, p)^{29}Si experiment of Hansen (private communication).
[b] "E_x" $=E_x(^{29}\text{Si})-8294$ keV.
[c] $E_x(^{29}P)=$"E_x" $+8376$ keV.
[d] Table I.
[e] Reference 7.
[f] From ^{30}Si(^{3}He, α)^{29}Si experiment of Dehnhard *et al.* (private communication).
[g] Table IV.

state of ^{29}P. Our analysis of both the resonance shapes in the elastic scattering and the decay schemes in the inelastic scattering strongly favored $l_p=2$ for both of the above-mentioned sharp resonances in ^{29}P, which ruled out both of them from being candidates for isospin $\frac{3}{2}$.

The fact that Dehnhard *et al.* had found the separation between the two $T=\frac{3}{2}$ states to be 1.340 MeV in ^{29}Si, rather than 1.406 MeV as in the parent ^{29}Al, and similar shifts between the positions of certain analog $T=1$ states in ^{24}Mg and ^{24}Na (Ref. 34), encouraged us to extend the region of our search downward in energy (see Figs. 18–22); we found only one sharp resonance at an excitation energy of 9.735 MeV (1.359 MeV above the ground-state analog resonance), which may have spin $\frac{1}{2}^+$. To decide definitely whether this sharp resonance is indeed the analog state, we will have to await a direct measurement of other properties of the second $T=\frac{3}{2}$ state in ^{29}P, such as via the ^{27}Al(^{3}He, n)^{29}P reaction, or by a ^{31}P(p, t)^{29}P experiment[4] with better statistics.

VIII. REDUCED WIDTHS

From the true *total* width of each resonance we have calculated a reduced width by dividing Γ by twice the penetrability $P_l=k/(F_l^2+G_l^2)$, where k is the wave number for the incident proton channel, and F_l and G_l are the regular and irregular Coulomb wave functions, respectively. (Since Γ_p/Γ is unknown for most of the $T=\frac{1}{2}$ resonances, we have taken $\Gamma_p=\Gamma$ for *all* resonances; these numbers should therefore be regarded as upper limits.) The values of the calculated reduced widths γ_λ^2 are listed in Tables VI and VII, along with the dimensionless reduced width θ_λ^2, obtained by dividing γ_λ^2 by the so-called "Wigner limit" $3\hbar^2/2ma_c$, where a_c is the channel radius, taken as 1.45 $(A^{1/3}+1)$fm. (A is the mass number of the target.)

In the R-matrix theory of nuclear reactions[35] the dimensionless reduced widths are defined as the integral of the product of channel and compound-nuclear wave functions over the channel surface. If the compound state has isospin $\frac{3}{2}$, and the channel wave function has isospin $\frac{1}{2}$, as in the cases under study, there will be no overlap between the wave functions, and the reduced widths vanish for all open channels. The fact that we have seen resonant effects in these channels implies that isospin is *not* a perfect quantum number, and some overlap does exist. This impurity arises both from a $T=\frac{1}{2}$ component in the compound-nuclear wave function, and a $T=\frac{3}{2}$ component in the channel wave function arising from a $T=1$ impurity in the target and residual nuclei. Calculations are now in progress at Rutgers[36] to predict these reduced widths using appropriate model wave functions, and treating the Coulomb interaction as a perturbation to the specifically nuclear interactions. This Coulomb perturbation may also explain the level shifts between analog states that we have observed in ^{25}Al and ^{29}P.

[34] P. Axel (private communication).

[35] A. M. Lane and R. G. Thomas, Rev. Mod. Phys. **30**, 257 (1958).

[36] J. N. Ginocchio (private communication); S. Yoshida (private communication).

TABLE VI. Reduced widths for ^{25}Al resonances.

E_x (MeV)	E_p (lab) (MeV)	Γ (lab) (keV)	l_p	T	γ_p^2 (MeV-cm)	$\theta_p^2=(2ma_c/3\hbar^2)\gamma_p^2$
7.662	5.601	50±15	3	$\frac{1}{2}$	4.2×10^{-14}	3.6×10^{-2}
7.863	5.811	20±8	1	$\frac{1}{2}$	3.3×10^{-15}	2.8×10^{-3}
7.916	5.866	<0.1	2	$\frac{3}{2}$	$<2.7\times10^{-17}$	$<2.0\times10^{-5}$
7.951	5.903	35±10	2	$\frac{1}{2}$	9.2×10^{-15}	7.8×10^{-3}
7.987	5.940	0.211±0.05	2	$\frac{3}{2}$	5.5×10^{-17}	4.7×10^{-5}
8.041	5.996	20±10	2	$\frac{1}{2}$	5.1×10^{-15}	4.3×10^{-3}
8.098	6.056	14.9±7	2	$\frac{1}{2}$	3.7×10^{-15}	3.2×10^{-3}
8.209	6.171	40±10	0	$\frac{1}{2}$	5.1×10^{-15}	4.3×10^{-3}

TABLE VII. Reduced widths for ^{29}P resonances.

E_x (MeV)	E_p (lab) (MeV)	Γ (lab) (keV)	l_p	T	γ_p (MeV-cm)	$\theta_p^2=(2ma_c/3\hbar^2)\gamma_L^2$
7.50	4.95	7±3	2	$\frac{1}{2}$	2.7×10^{-15}	2.4×10^{-3}
7.74	5.19	~2	2	$\frac{1}{2}$	6.9×10^{-16}	6.0×10^{-4}
8.08	5.55	36±10	2	$\frac{1}{2}$	1.1×10^{-14}	9.8×10^{-3}
8.20	5.67	20±4	2	$\frac{1}{2}$	5.7×10^{-15}	2.3×10^{-3}
8.376	5.840	0.168±0.05	2	$\frac{3}{2}$	2.5×10^{-17}	2.3×10^{-5}
8.51	5.99	25±7	2	$\frac{1}{2}$	6.4×10^{-15}	5.8×10^{-3}
8.89	6.39	33±6	2	$\frac{1}{2}$	7.5×10^{-15}	6.8×10^{-3}
9.540	7.046	50±10	0	$\frac{1}{2}$	5.9×10^{-15}	5.4×10^{-3}
9.617	7.126	40±10	0	$\frac{1}{2}$	4.7×10^{-15}	4.2×10^{-3}
9.652	7.162	8.6±3	3	$\frac{1}{2}$	3.3×10^{-15}	3.0×10^{-3}
9.735	7.248	6.5±3	0	$\frac{3}{2}$?	7.5×10^{-16}	6.8×10^{-4}
9.753	7.266	7.6±3	2	$\frac{1}{2}$	1.4×10^{-15}	1.3×10^{-3}
9.765	7.279	7.6±3	2	$\frac{1}{2}$	1.4×10^{-15}	1.3×10^{-3}
9.807	7.322	19.8±10	2	$\frac{1}{2}$	3.6×10^{-15}	3.3×10^{-3}
9.864	7.381	11.7±5	2	$\frac{1}{2}$	2.1×10^{-15}	1.9×10^{-3}

TABLE VIII. Excitation energies and masses of the members of the quartets.

	$A=25$			$A=29$		
T_z	Nucleus	E_x (keV)	$M(T=\frac{3}{2})-25$ (keV)	Nucleus	E_x (keV)	$M(T=\frac{3}{2})-29$ (keV)
			Measured			Measured
$\frac{3}{2}$	^{25}Na	0.0	−9356±9	^{29}Al	0.0	−18 218±6
$\frac{1}{2}$	^{25}Mg	7812±25	−5379±25	^{29}Si	8294±10	−13 600±11
$-\frac{1}{2}$	^{25}Al	7916±6	−1015±9	^{29}P	8376±6	−8 569±9
			Calculated			Calculated
$-\frac{3}{2}$	^{25}Si	0.0	3735±80[a]	^{29}S	0.0	−3 126±43[a]

[a] These uncertainties were given incorrectly in Ref. 25. See Phys. Letters **27B**, 18E (1968). Mass values obtained from Isobaric Mass Formula (see Sec. IX).

TABLE IX. Coulomb energy differences for isospin quartets with $A=25$ and 29.

M_2-M_1	$\Delta E_c-\delta$ (keV)		$\Delta E_c^{\text{exptl}}$ (keV)		$\Delta E_c^{\text{calc a}}$ ($r_0=1.45$fm) (keV)	$\Delta E_c^{\text{calc a}}$ ($r_0=1.36$fm) (keV)
	1st Quar.	2nd Quar.	1st Quar.	2nd Quar.		
^{25}Mg–^{25}Na	3977	...	4759	...	4484	4780
^{25}Al–^{25}Mg	4364	...	5146	...	4890	5214
			387[b]			
^{29}Si–^{29}Al	4618	4552	5400	5334	5039	5373
^{29}P–^{29}Si	5031	5050	5813	5832	5427	5786
			413[b]	498[b]		

[a] $\Delta E_c(Z)=E_c(Z+1)-E_c(Z)=(6e^2/5r_0)(Z/A^{1/3})$.

[b] Second Coulomb-energy difference: $\Delta_2(Z)\equiv\Delta E_c(Z)-\Delta E_c(Z-1)$.

IX. MASSES OF ^{25}Si AND ^{29}S

With the improved accuracy of our values for the excitation energies of the $T=\frac{3}{2}$ states in the $T_z=-\frac{1}{2}$ members of the mass-25 and -29 isospin quartets, we were able to use the isobaric multiplet mass formula[37]

$$M(A,T,T_z)=a(A,T)+b(A,T)T_z+c(A,T)T_z^2,$$

where a, b, and c are constants for a given multiplet, to calculate the masses of the $T_z=-\frac{3}{2}$ members of these quartets. These predictions are listed in Table VIII, which includes the precision data of Hansen *et al.*[30] from the ^{27}Al(^{3}He, p)^{29}Si reaction. Our predictions may be compared with those of the semiempirical (independent-particle model) mass formula of Garvey and Kelson[38] which yields 3770 and -3020 keV for the mass defects of ^{25}Si and ^{29}S, respectively. A careful, independent determination of the masses of these nuclei by experiments such as (^{3}He, ^{6}He) reactions[39] on ^{28}Si and ^{32}S is very desirable in order to put stringent limits on any possible T_z^3 terms in the isobaric mass formula.

X. COULOMB ENERGY DIFFERENCES

We have calculated Coulomb energy differences between neighboring members of the $A=25$ and 29 isospin quartets which are listed in Table IX. Using a uniform charge distribution for the nucleus gives a value of $(6/5)(e^2/r_0)Z/A^{1/3}$ for the Coulomb energy difference between isobars having $Z+1$ and Z protons, where e is the electron charge, and r_0 the proportionality constant between the charge radius and $A^{1/3}$. Calculated values for this simple model are also listed in the table for $r_0=1.45$ fm, and $r_0=1.36$ fm.

Referring to Table IX, we notice a change in the Coulomb energy differences between ^{29}Si and ^{29}Al, and between ^{29}P and ^{29}Si as we go from the first isospin quartet to the second quartet. This shift is unexpected in the usual theory of isobaric analog states,[40] but it may be expected that the Coulomb perturbation which produces isospin mixing of the wave functions of the compound nucleus is also responsible for the shifts in the positions of these energy levels. Zamick[41] attempted to explain the discrepancy between the 71-keV separation of the analog resonances in ^{25}Al and the 90-keV separation in the parent ^{25}Na; the differences in the Coulomb interaction between three $d_{5/2}$ proton holes in ^{28}Si (model of ^{25}Na), as opposed to only one $d_{5/2}$ proton hole for ^{25}Al, has led to a calculated shift in a direction opposite to what we observed experimentally. More detailed calculations of this shift are in progress.[42]

ACKNOWLEDGMENTS

We gratefully acknowledge the assistance of the following people in various phases of this investigation: J. P. F. Sellschop from the University of Witwatersrand, South Africa, for helpful advice; G. T. Garvey of Princeton for keeping us up-to-date on developments in the use of isospin in nuclear physics; O. Hansen, who even after his return to Copenhagen followed the progress of our research, and who performed several valuable measurements which considerably aided us in some of our work; G. H. Lenz, H. Ogata, E. J. Schneid, R. Van Bree, and M. Wiesen for help in taking the

[37] E. P. Wigner and E. Feenberg, Repts. Prog. Phys. **8**, 274 (1941); S. Weinberg and S. B. Treiman, Phys. Rev. **116**, 465 (1959).

[38] G. T. Garvey and I. Kelson, Phys. Rev. Letters **16**, 197 (1966); I. Kelson and G. T. Garvey, Phys. Letters **23**, 689 (1966).

[39] J. Cerny, R. H. Pehl, G. Butler, D. G. Fleming, C. Maples, and C. Detraz, Phys. Letters **20**, 35 (1966).

[40] D. Robson, Phys. Rev. **137**, B535 (1965).

[41] L. Zamick (private communication).

[42] S. Yoshida, G. Ripka, and L. Zamick (private communications).

data; R. Klein for preparing the targets; R. Van Bree for making his data-processing computer programs available; G. Ripka and L. Zamick for helpful discussions on the theoretical aspects; and G. C. Morrison, R. E. Segel, and D. H. Youngblood of Argonne National Laboratory, with whom we maintained close contact during our concurrent searches for these elusive resonances.

APPENDIX A: TARGET PREPARATION

We present here some techniques developed to overcome some of the problems involved in preparing thin targets of Mg and Si. We used magnesium leaf[43] enriched to 99.88% in ^{24}Mg, with 0.09% ^{25}Mg and 0.03% ^{26}Mg impurities. In order to prevent the Mg leaves from splattering out of the tantalum crucible upon heating under high vacuum in a bell jar, we used Ta powder as ballast, since the Ta did not evaporate at the vaporization point of Mg. We found that after evaporation, the Mg vapor would not condense on the usual sugar or meta-phosphate substrates or carbon backings. We therefore seeded the slides with trace amounts of Au or Ag prior to evaporation of the Mg. Finally, in order to prevent the Mg targets from rapidly oxidizing, as indicated by a wrinkled, tarnished appearance, we thoroughly dried the carbon backings in a desiccator for at least one hour before evaporating the Mg directly onto the carbon films previously floated onto target holders. The oxide contaminant then appeared to be only a surface layer, as the yield from the oxygen impurity remained fairly constant, independent of the Mg thickness.

We evaporated natural SiO to make thin ^{28}Si targets, after trying unsuccessfully to evaporate enriched SiO_2. The major problem which we encountered was that of overheating the substrates during evaporation, which caused the films to disintegrate in water when the substrates were floated from the slides. We overcame this problem by placing the substrates at large distances from the crucible, by the use of pure quartz slides, by using Cu as a substrate which was later etched away, and by performing the evaporation rapidly to avoid overheating. The ^{29}Si (4.70%) and ^{30}Si (3.09%) impurities introduced an additional uncertainty of about 6% in the absolute cross sections for proton scattering from ^{28}Si. We normalized our cross-section data by repeating a portion of the excitation curve around the sharp resonance at $E_p=4.884$ MeV, measured by Belote *et al.*,[26] and assumed, as they did, that the number of particles scattered elastically from ^{28}Si was simply 92.2% of the total number of elastically scattered particles in the Si peak. For the ^{24}Mg+p data, we repeated a flat portion of the elastic scattering cross sections at 164° from 3.70 to 3.90 MeV, measured at Wisconsin by Mooring *et al.*[8]

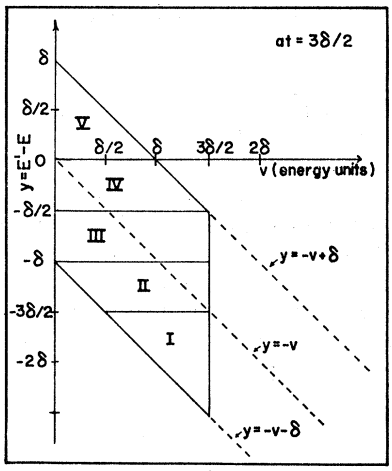

FIG. 23. Region of integration in the y-v plane. Boundaries shown are for the case where the target thickness at is 1.5 times the beam spread δ.

APPENDIX B: EFFECTS OF IMPERFECT ENERGY RESOLUTION

It is impossible to perform a scattering-cross-section measurement at one precise energy, even though it would be desirable to do so. Several factors act to produce a spread of energies in the particles available for collisions with the target nuclei, the most important of which are the distribution of energies in the accelerated beam, and the energy losses in the target. Therefore, when trying to extract quantitative information from cross-section data, one cannot simply compare the theoretical cross section calculated at one energy with the cross section measured at that energy, but one must average the theory in order to take into account the effects of imperfect energy resolution.

For the energy distribution of protons in the beam, we define a function $g(E-E')$ such that $g(E-E')dE'$ represents the fraction of incident protons with energies between E' and $E'+dE'$, where E is the energy determined from the NMR frequency. This function is assumed to be triangular[44] and is normalized. After a proton of energy E has penetrated a distance x into the target, its energy has decreased to the value $E-ax$, where a is the stopping power of the target material. The energy distribution of protons at the depth x in the target is thus $g(E-v-E')$, where $v=ax$.

Following Koester's treatment,[45] the measured differ-

[43] Purchased from Stable Isotopes Division, Oak Ridge National Laboratory, Oak Ridge, Tenn.

[44] R. G. Herb, S. C. Snowdon, and O. Sala, Phys. Rev. **75**, 246 (1949).

[45] L. J. Koester, Phys. Rev. **85**, 643 (1952).

ential cross section at the nominal energy E and angle θ is

$$\sigma_0(E,\theta)=(at)^{-1}\int_0^{at}dv\int_{E-v-\delta}^{E-v+\delta}g(E-v-E')\sigma(E',\theta)\,dE',$$

where at is the target thickness in energy units, δ is the maximum deviation of protons in the beam from energy E, and $\sigma(E',\theta)$ is the theoretical cross section at the energy E'. Since the cross section is not a simple function of energy, it is convenient to change the order of integration and perform the integration over v first. This results in an expression of the form

$$\sigma_0(E,\theta)=(at)^{-1}\int_{E-\delta-at}^{E+\delta}\sigma(E',\theta)F(E'-E)\,dE',$$

where we now wish to explicitly evaluate the function $F(E'-E)=F(y)$, where $y\equiv E'-E$.

The triangular function g is separated conveniently into two pieces:

$$g_L=(1/\delta)^2(y+\delta+v)\quad\text{when}\quad -\delta-v\leq y\leq -v,$$

and

$$g_R=(1/\delta)^2(-y+\delta-v)\quad\text{when}\quad -v\leq y\leq +\delta-v.$$

The region of integration lies in the y-v plane, and the boundaries of this region are shown in Fig. 23. The integral over v must be broken up into five parts, the points at which the breaks occur depending on the value of the target thickness at. Three different cases must be considered:

Case I: $0\leq at\leq\delta$

$$F(y)=\delta^{-2}\times$$

$\frac{1}{2}(y+\delta)^2+at(y+\delta)+\frac{1}{2}(at)^2$	$-at-\delta\leq y\leq-\delta$
$at(y+\delta)+\frac{1}{2}(at)^2$	$-\delta\leq y\leq-at$
$-y^2-aty+\delta at-\frac{1}{2}(at)^2$	$-at\leq y\leq 0$
$at(-y+\delta)-\frac{1}{2}(at)^2$	$0\leq y\leq-at+\delta$
$\frac{1}{2}(-y+\delta)^2$	$-at+\delta\leq y\leq\delta$;

Case II: $\delta\leq at\leq 2\delta$

$$F(y)=\delta^{-2}\times$$

$\frac{1}{2}(y+\delta)^2+at(y+\delta)+\frac{1}{2}(at)^2$	$-at-\delta\leq y\leq-t$
$-\frac{1}{2}y^2+(\delta-at)y+\frac{1}{2}\delta^2+\delta at-\frac{1}{2}(at)^2$	$-at\leq y\leq-\delta$
$-y^2-aty+\delta at-\frac{1}{2}(at)^2$	$-\delta\leq y\leq-at+\delta$
$-\frac{1}{2}y^2-\delta y+\frac{1}{2}\delta^2$	$-at+\delta\leq y\leq 0$
$\frac{1}{2}(-y+\delta)^2$	$0\leq y\leq\delta$;

Case III: $2\delta\leq at$

$$F(y)=\delta^{-2}\times$$

$\frac{1}{2}(y+\delta)^2+at(y+\delta)+\frac{1}{2}(at)^2$	$-at-\delta\leq y\leq-at$
$-\frac{1}{2}y^2+(\delta-at)y+\frac{1}{2}\delta^2+\delta at-\frac{1}{2}(at)^2$	$-at\leq y\leq-at+\delta$
δ^2	$-at+\delta\leq y\leq-\delta$
$-\frac{1}{2}y^2-\delta y+\frac{1}{2}\delta^2$	$-\delta\leq y\leq 0$
$\frac{1}{2}(-y+\delta)^2$	$0\leq y\leq\delta$.

It can be easily verified that the function $F(y)$ is properly normalized to area at, and $F(y)$ agrees with the plot in Ref. 45 for the special case $\delta=at$.